Biomedicine & Pharmacotherapy 109 (2019) 1211–1220

Contents lists available at ScienceDirect

Biomedicine & Pharmacotherapy

journal homepage: www.elsevier.com/locate/biopha

Safety, pharmacokinetics, and prevention effect of intraocular crocetin in proliferative vitreoretinopathy

Hui-Fang Wang[a,b], Jing-Xue Ma[a,*], Qing-Li Shang[a], Jian-Bin An[a], Hai-Ting Chen[a,c], Cai-Xia Wang[a]

[a] Department of Ophthalmology, The Second Hospital of HeBei Medical University, Shijiazhuang, 050000, China
[b] Department of Ophthalmology, Shijiazhuang Aier Eye Hospital, Shijiazhuang, 050000, China
[c] Department of Ophthalmology, Cangzhou Central Hospital, Cangzhou, 061000, China

ARTICLE INFO

Keywords:
Crocetin
PVR
Toxicity
Pharmacokinetics
HPLC

ABSTRACT

The study was designed to determine the safety and pharmacokinetics of intraocular crocetin and examine whether crocetin inhibits the development of proliferative vitreoretinopathy (PVR) in a rabbit model. In the toxicity study, the right eyes of rabbits were injected with 0.2 μmol or 0.4 μmol crocetin. The left eyes were injected with 0.1 ml phosphate buffered saline (PBS) containing the same concentration of DMSO. Fundus photography, optical coherence tomography (OCT), and electroretinogram (ERG) were obtained at baseline and 14 days. Afterward, the eyes were enucleated for histopathological analysis and terminal deoxynucleotidyl transferasemediated dUTP nick end labeling (TUNEL) assay. In the pharmacokinetic study, the eyes received an intravitreous injection of 0.4 μmol crocetin to detect vitreous drug levels with HPLC at specific time points. In the efficacy study, PVR was induced with an intravitreal injection of ARPE-19 cells in rabbits. Then ten eyes were injected with 0.4 μmol crocetin, and the other 10 eyes received 0.1 ml PBS. Fundus photography, OCT and ERG were performed at days 3 and 7 and weekly for a total of 4 weeks after injection. Afterward, the eyes were enucleated and subjected to histological analysis and TUNEL staining. The results demonstrated no signs of retinal toxicity. Intravitreal injection of 0.4 μmol crocetin had a half-life of 4.231 h. Treatment with crocetin significantly inhibited the progression of PVR in parallel with a reduced expression of α-SMA, collagen fibers and Ki67. These results indicate that crocetin is an effective and safe inhibitor of PVR in rabbit models.

1. Introduction

Proliferative vitreoretinopathy (PVR), as a cause of common failure, occurs after 5% to 10% of rhegmatogenous retinal detachment surgeries [1]. PVR pathogenesis is a complex wound healing process involving excessive cellular proliferation and migration, extracellular matrix (ECM) production and membrane formation. The major cell types involved in PVR are RPE, glial cells and fibroblasts [2]. Many growth factors, receptors and their downstream signaling pathway mediators have been described in patients and experimental animal models suffering from PVR.

The separation of the neuroretina from the RPE and the loss of cell-to-cell contact trigger the quiescent RPE cells to proliferate and transform. The isolated RPE cells lose their epithelial morphology, migrate into the vitreous and respond to proliferating factors, such as platelet derived growth factor (PDGF), fibroblast growth factor (FGF), epidermal growth factor (EGF), insulin-like growth factor (IGF), vascular endothelial growth factor (VEGF), hepatocyte growth factor (HGF), and transforming growth factor β (TGF-β). In this process, the RPE cells undergo epithelial-mesenchymal transition (EMT) and become fibroblast- or myofibroblast-like cells acquiring enhanced capacities of migration, invasiveness, and extracellular matrix production [3].

Along with the advances in vitrectomy for patients with PVR, the anatomical results after surgery have improved in recent years. However, the functional recovery remains unsatisfactory. There is a need to explore pharmacological adjuvant treatment that could prevent or halt the progression of PVR. To date, pharmacological strategies tested in experimental and clinical studies have included anti-inflammatory components (steroids such as triamcinolone acetonide and methylprednisolone acetate) [4,5], anti-proliferative components (e.g., 5-FU, daunorubicin, Taxol, colchicine, retinoic acid, ribozymes, vincristine, cisplatin, adriamycin, mitomycin, and dactomycin) [6,7], anti-growth factors (e.g., SU9518 and AG1295, PDGFR kinase inhibitor and LY-364947, a TGF-β receptor 1 inhibitor) [8–10], a combinatorial approach (combination of 5-FU and low-molecular-weight heparin) [11] and several natural products, (e.g. resveratrol) [12]. However, most of

* Corresponding author.
E-mail address: majingxue2000@163.com (J.-X. Ma).

https://doi.org/10.1016/j.biopha.2018.10.193
Received 17 July 2018; Received in revised form 31 October 2018; Accepted 31 October 2018

these attempts are unsatisfactory. More attempts to identify effective pharmacological treatments for PVR are still needed.

Crocetin (8, 8′-diapocarotene-8, 8′-dioic acid) belongs to the family of carotenoids and is a major component of saffron [13]. Crocetin represents several biological activities, including growth inhibitory or pro-apoptotic properties in several malignant cells (pancreatic, esophageal and colorectal cancer cells) [14–16], preventing ischemia and N-methyl-D-aspartate -induced retinal damage [17,18], and antifibrotic effects in scleroderma fibroblasts and in sclerotic mice [19]. Our previous study demonstrates that crocetin is an effective inhibitor of the proliferation, migration and TGF-β_2-mediated EMT of ARPE-19 cells in an in vitro PVR model [20]. In the present study, we evaluated the inhibitory effect of crocetin on rabbit models of PVR at nontoxic doses.

2. Materials and methods

2.1. Animals

Pigmented rabbits, each weighing 2.5–3 kg, were used in this study. All of the animal experiments adhered to the National Institutes of Health guide for the care and use of Laboratory animals and were approved by the Animal Care and Use Committee of Hebei Medical University. All of the procedures were performed under intravenous anesthesia with 2% pentobarbital at 1 ml/kg.

2.2. Cell culture

The human RPE cell line ARPE-19 was obtained from the American Type Culture Collection (ATCC, Manassas, VA, USA) and cultured in DMEM/F12 supplemented with 10% fetal bovine serum (FBS, Gibco, Grand Island, NY, USA), 100 U/ml penicillin and 100 μg/ml streptomycin in a humidified atmosphere at 37 ℃ in 5% CO_2. ARPE-19 cells at passages 7–20 were used to induce PVR in rabbits.

2.3. Intravitreal injection of crocetin for the toxicity study

Crocetin (MP Biomedicals, Santa Ana, CA, USA) was acquired in powder form and dissolved in dimethyl sulfoxide (DMSO, Sigma-Aldrich, St. Louis, MO, USA). Next, crocetin was suspended in 0.1 ml phosphate buffered saline (PBS) at concentrations of 0.2 μmol/0.1 ml and 0.4 μmol/0.1 ml. The right eye (four eyes per concentration) of each animal was injected with 0.1 ml of a drug concentration, and the corresponding left eye (control) was injected with 0.1 ml PBS containing the same concentration of DMSO alone.

The animals were anesthetized with an intravenous injection of 1 ml/kg 2% pentobarbital (Sigma-Aldrich, St. Louis, MO, USA). Corneal anesthesia (0.5% proparacaine hydrochloride ophthalmic eye drops, Alcon Laboratories, Inc., Fort Worth, TX, USA) was applied after pupil dilation with topical use of tropicamide (5%) and phenylephrine (5%) eye drops (Shenyang Sinqi Pharmaceutical Co., Shenyang, China). Next, 0.1 ml vitreous was removed with a 25-gauge needle 4 mm posterior to the corneal limbus. Subsequently, 0.1 ml PBS with or without crocetin was injected into the vitreous with a 30-gauge needle linked to a 1 ml insulin syringe.

2.4. Ophthalmologic examinations

The animals underwent eye examinations before injection and at 1, 3, 5, 7, and 14 days through slit-lamp biomicroscopy and indirect ophthalmoscopy. Special examinations, such as digital fundus camera (ZEISS, Oberkochen, Germany), optical coherence tomography (OCT, Heidelberg Engineering, Inc., Heidelberg, Germany), and electroretinogram (ERG, Metrovision, Perenchies, France), were conducted before injection and at 14 days.

2.5. ERG

For the functional study, full-field ERG was performed by adhering to the International Society for Clinical Electrophysiology of Vision (ISCEV) standards in both eyes before and 7, 14 days after injection [21]. The animals were dark adapted for at least 30 min and anesthetized. The pupils were fully dilated, and the eyes were topically anesthetized. An active electrode was placed on the cornea. The reference and ground silver needle electrodes were positioned subcutaneously in the forehead. After a 30 min of dark adaptation, the scotopic ERG was recorded, including an isolated rod (scotopic 0.01 ERG), standard flash (maximal) response (scotopic 3.0 ERG), and oscillatory potentials (scotopic 3.0 OPs). After a 10-minute light adaptation, the photopic ERG was obtained including a single white flash (photopic 3.0 ERG) and a 30 Hz flicker (photopic 3.0 flicker).

The ERG analysis was based on the changes of a- and b-wave amplitudes in scotopic ERG and photopic ERG before and after injection. A-wave amplitudes were measured from the prestimulus baseline to the trough of the negative wave, and b-wave amplitudes were measured from the trough of the a-wave to the peak of the b-wave.

2.6. Pharmacokinetic study

2.6.1. Sample preparation

Both eyes of fourteen pigmented rabbits received an intravitreous injection of 0.4 μmol crocetin as described above. The rabbits were euthanized immediately and at 1, 3, 7, 12, 24, 48, and 72 h after injection. The eyes were then enucleated and immediately flash frozen at −80 ℃. The frozen eyes were dissected, and the entire vitreous was isolated with complete removal of the sclera, choroid, and retina.

Soluble and insoluble crocetin present in the vitreous was processed as follows. The vitreous was centrifuged at 10,000 rpm for 10 min to separate the supernatant and the pellet. The supernatant was pipetted out, and the volume was measured. For estimation of the soluble crocetin, 0.2 ml of supernatant of the vitreous with 0.2 ml methanol containing 3.5 μg/mL of the internal standard (curcumin) was added to tubes and vortexed for 2 min on a multiple vortexer. Subsequently, the mixture was centrifuged for 10 min at 10,000 rpm to separate the tissue proteins. The resulting supernatant was pipetted out, dried under a nitrogen stream at 40 ℃, and reconstituted with 0.2 ml methanol before analysis with an HPLC system. For estimating the insoluble crocetin, the insoluble particles obtained from the centrifugation of the vitreous was added with 0.4 ml methanol containing 8.775 μg/mL of internal standard (curcumin) and was vortexed for 5 min to dissolve the crocetin. Subsequently, the samples were dried under a nitrogen stream at 40 ℃ and reconstituted with 0.1 ml methanol before analysis with a high-performance liquid chromatography (HPLC) system.

2.6.2. High-performance liquid chromatography (HPLC)

HPLC analysis was performed on a gradient HPLC pump (e2695, Waters, Milford Massachusetts, USA) equipped with an optical detector (2489 UV/Vis Detector; Waters, Milford Massachusetts, USA). The mobile phase was methanol-water-acetic acid (84:16:0.34, volume to volume) with a flow rate of 1.0 ml/min. A 20-μL volume of each sample was separated through a C18 Column (5 μm, 250 mm × 4.6 mm; Dikma Science, China), with the column temperature being maintained at 35 ℃. Crocetin and curcumin (the internal standard) were monitored by ultraviolet absorbance at 423 nm, and no interference was observed from the sample background. Crocetin was observed to have a t_R of 8.3 min, whereas curcumin had a t_R of 4.8 min. Two standard curves covered the range from 0.2 μg/mL to 40 μg/mL for soluble crocetin (correlation coefficient 0.9996) and from 0.2 μg/mL to 400 μg/mL for insoluble crocetin (correlation coefficient 0.9996).

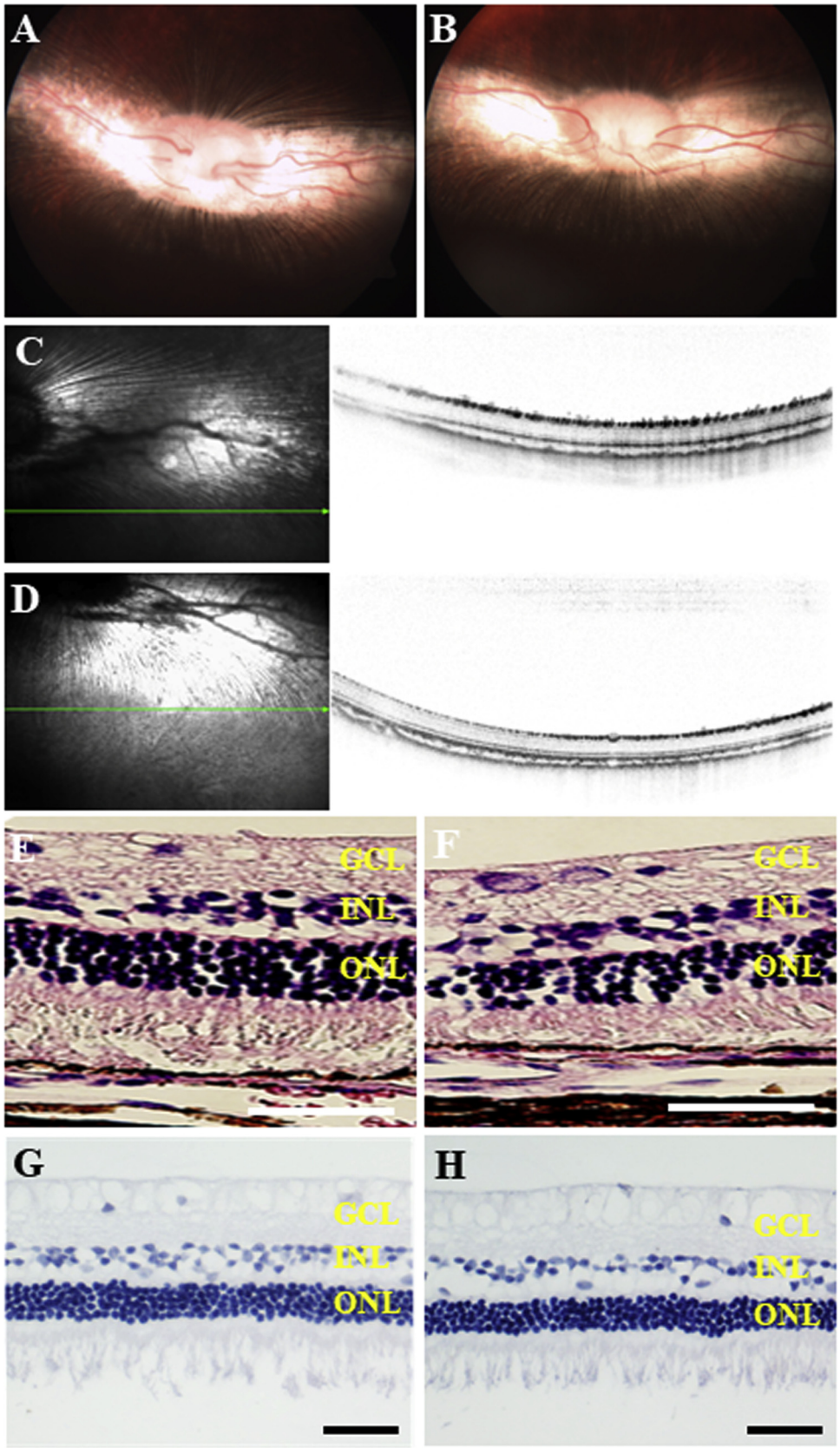

Fig. 1. Funduscopy, OCT, micrographs and TUNEL staining of the retinal Section 2 weeks after the injection of 0.4 μmol crocetin (A, C, E and G) and vehicle (B, D, F and H). The crocetin-treated right eyes and vehicle-treated left eyes both demonstrated no signs of retinal atrophy or necrosis by funduscopy and OCT (A, B, C, and D). Light microscopy of retinal sections showed complete preservation of all retinal layers (E and F). TUNEL staining showed no signs of cell apoptosis in two groups (G and H). GCL-ganglion cell layer, INL-inner nuclear layer, ONL-outer nuclear layer, scale bar: 20 μm.

2.7. Efficacy study

2.7.1. PVR induction in rabbits

PVR was induced in the right eye of twenty pigmented rabbits following a reported protocol [12]. Briefly, after 0.2 ml of vitreous was removed with a 25-gauge needle, 0.1 ml PBS with (10 eyes) or without (10 eyes) 0.4 μmol crocetin and accompanied by 0.1 ml DMEM/F12 containing 2×10^5 ARPE-19 cells and 50 ng PDGF-BB (R&D Systems, Minneapolis, MN, USA) were injected into the vitreous cavity 4 mm posterior to the corneal limbus with a 1 -ml insulin syringe. Eyes with complications, such as vitreous hemorrhage and cataract formation, were eliminated from the study. The clinical examinations with a digital fundus camera, OCT, and ERG were performed at days 3 and 7 and weekly for a total of 4 weeks after injection. The stage of PVR was graded according to Fastenberg classification from 0 through 5 at days 7, 14, and 28 after injection [22].

2.7.2. Histopathological examination (hematoxilin-eosine, Masson's trichrome and immunohistochemical staining)

On day 28 after cell injection, the animals were euthanized under anesthesia with an overdose administration of intravenous 2% pentobarbital, and the eyes were enucleated for the histological analysis. Enucleated globes were fixed for 2 h in 4% paraformaldehyde (PFA) (pH 7.4) and were cut immediately posterior to the ora serrata to remove the anterior segment. The eye cups were further fixed for 36–48 h in 4% PFA. The degree of pathological gross changes of PVR was recorded with a camera. The eyes were then embedded in paraffin. A 5-μm cross-section thickness involving the pupil and the optic nerve was prepared. The retinal sections were stained with Masson's trichrome and hematoxilin-eosine (H&E) as previously described.

Immunohistochemistry was performed with a two-step indirect staining as previously described. In brief, the retinal sections were incubated with 0.3% H_2O_2 in 0.1% sodium azide for 10 min to block endogenous peroxide. Following a 30 min heat-mediated antigen retrieval, the sections were blocked in 10% normal goat serum for 1 h to avoid non-specific antibody binding and were incubated with monoclonal antibody for detection of α-SMA (cat. no. ab7817, Abcam, Cambridge, UK) or polyclonal antibody for detection of Ki67 (cat. no. ab15580, Abcam, Cambridge, UK) overnight at 4 °C. After washing with PBS, the slides were incubated with biotinylated IgG (cat. no. ab6788 or ab64256, Abcam, Cambridge, UK) for 1 h and with 3, 3'-diaminobenzidine (DAB) for 10 min. before counterstaining with hematoxylin.

2.7.3. Terminal deoxynucleotidyl transferase-mediated dUTP nick end labeling (TUNEL) assay

Apoptotic cells in retina were detected by the TUNEL assay using an in situ cell death detection kit POD (No. 11684817910; Roche, Switzerland) according to the manufacturer' s instructions.

2.8. Data analysis

All of the data are expressed as the mean ± standard deviation and were analyzed using SPSS version 16.0 (SPSS, Inc., Chicago, IL). The elimination half-life ($t_{1/2}$) was calculated with DAS version 3.0 (BioGuider Co., Shanghai, China). The statistical significance was determined using a two-tailed Student's *t*-test or Mann-Whitney *U* test (nonparametric data). *P*-values less than 0.05 were considered to be significant.

3. Results

3.1. Toxicity

3.1.1. Clinical observations, histology and TUNEL staining

All of the animals (8 rabbits) accepted the intravenous injection with no signs of pain under anesthetics. There were no cases of retinal detachment or intraocular inflammation. One left eye and one right eye were excluded from the study for vitreous hemorrhage and cataract formation, respectively. Indirect ophthalmoscopy and OCT demonstrated no signs of retinal hemorrhage, edema, or optic nerve pallor (Fig. 1A–D). Histological examination in H&E staining showed complete preservation of all retinal layers in both the experimental eyes and the control eyes (Fig. 1 E, F). There was no sign of atrophy or necrosis in the inner and outer retina. The sections represented the same degree of mild vacuolization in the ganglion cell layer in both the treated and control eyes. This finding might be attributable to autolysis and tissue processing artifacts. TUNEL staining showed that intravitreal injection of crocetin up to 0.4 μmol did not induce cell apoptosis compared with the control group (Fig. 1G, H).

3.1.2. ERG

Under scotopic testing conditions, there was no significant difference in a-wave and b-wave amplitudes between crocetin-injected right eyes and vehicle-injected left eyes at any time point. Under photopic testing conditions, there was a decrease in the a-wave amplitude at 1 week in 0.4 μmol crocetin-injected right eyes, but the decrease had no significant difference compared with the left eyes and returned to normal at 2 weeks. No difference in a-wave and b-wave amplitudes was found between crocetin-injected right eyes and vehicle-injected left eyes at any time point.

3.2. Pharmacokinetics

The mean crocetin concentrations and insoluble crocetin amount in the vitreous at specific time points after intravitreal injection with 0.4 μmol/0.1 ml are listed in Table 3. The highest concentration of crocetin in the vitreous was 36.77 ± 3.39 μg/ml (111.98 μM) observed 1 h after intravitreal administration and it declined to 11.13 ± 0.02 μg/ml (33.89 μM) at 7 h and 1.89 ± 0.04 μg/ml (5.77 μM) at 24 h, separately. The observed concentration-time data for crocetin at seven time points is presented in Fig. 2. The half-life of intravitreal injection of 0.4 μmol crocetin was 4.231 h calculated using a non-compartmental model.

3.3. Efficacy of crocetin in the PVR model

Next, we investigated whether crocetin can influence the pathogenesis of PVR in vivo using a rabbit model of PVR. The Mann-Whitney U Test for nonparametric data showed a statistically significant differences ($P < 0.05$) at days 14, and 28 between the experimental and

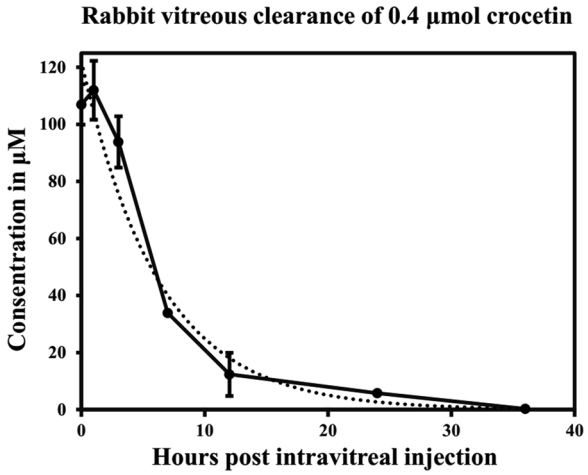

Fig. 2. Crocetin pharmacokinetics in the vitreous after intravitreal injection of 0.4 μmol in the rabbit. Concentrations of crocetin at 0.4 μmol follow a one-phase decay model.

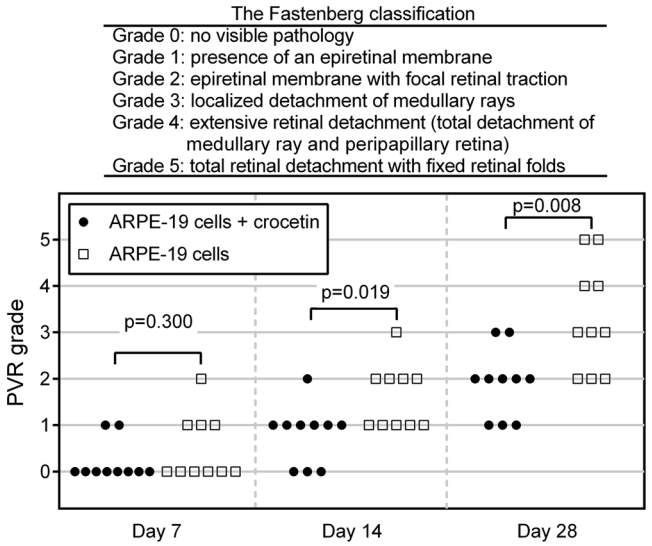

Fig. 3. Inhibition effect of crocetin on the progression of PVR stages in rabbit models injected with ARPE-19 cells + PBS or ARPE-19 cells + 0.4 μmol crocetin. The classification of the PVR grade used in this study was listed at the top. Mann-Whitney analysis showed a statistically significant difference at day 14 and day 28 between two groups. **P < 0.01. *P < 0.05. n = 10/group.

control groups (Fig. 3).

On the seventh day after injection, ARPE-19 cells with PBS had already formed endovitreous fibrotic membranes, whereas ARPE-19 cells with crocetin remained as cell aggregates in the vitreous. PVR progressed more seriously in the eyes injected with ARPE-19 cells + PBS than those injected with ARPE-19 cells + 0.4 μmol crocetin for up to 28 days. On day 28, seven of ten rabbits experienced retinal detachment in the control group (2 in stage 5, 2 in stage 4, and 3 in stage 3). Representative fundus pictures and OCT showed extensive retinal detachment with a fixed retinal fold. In contrast, only 2 in 10 rabbits in the experimental group appeared with localized detachment of medullary rays in stage 3. Five in ten showed focal traction and engorgement in stage 2 (Fig. 4).

The eyeball without the anterior segment was photographed to observe the macroscopic pathology. A globe from the control group showed complete tractional retinal detachment (TRD) (Fig. 5A2). A globe from the experiment group showed a partial TRD with detachment of the medullary ray (Fig. 5A3). A normal eye with macroscopic pathology (Fig. 5A1), HE stain of the retina (Fig. 5B1), immunohistochemical stain of the retina and optic nerve for α-SMA (Fig. 5C1 and D1), and Masson's trichrome stain for collagen (Fig. 5E1) was listed on the left row of Fig. 5. Histological findings confirmed the formation of epiretinal fibrotic membranes in two groups in different severity. In the eyes injected with ARPE-19 cells + PBS, fibrotic membranes with dense collagen fibers and cells were drawn up through the retina and made it convoluted (Fig. 5B2). In contrast, the eyes injected

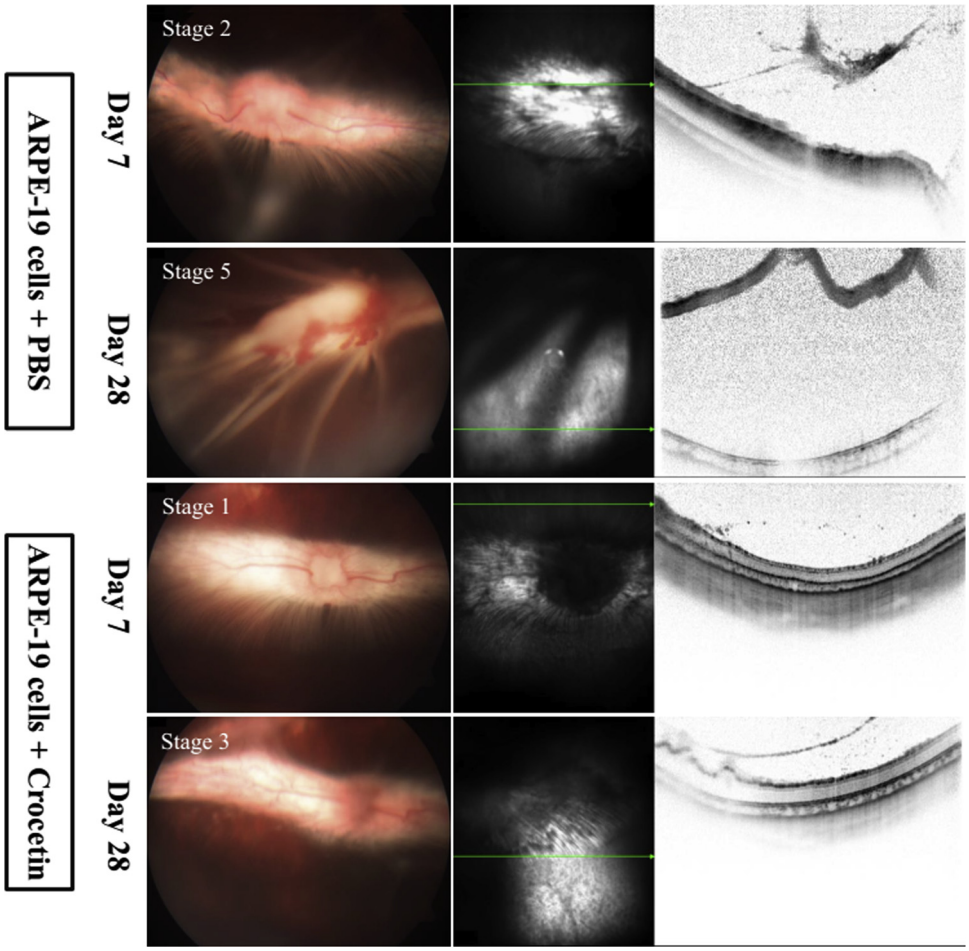

Fig. 4. Ocular fundus photographs and OCT images of eyes with PVR after treatment with ARPE-19 cells + PBS or ARPE-19 cells + 0.4 μmol crocetin. Eyes injected with ARPE-19 cells + PBS formed a fibrous membrane with focal retinal traction (stage 2) at day 7 and developed total retinal detachment (stage 5) at day 28. The eyes injected with ARPE-19 cells + 0.4 μmol crocetin remained in the cell cluster (stage 1) at day 7 and appeared as localized detachment of the medullary ray (stage 3) at day 28.

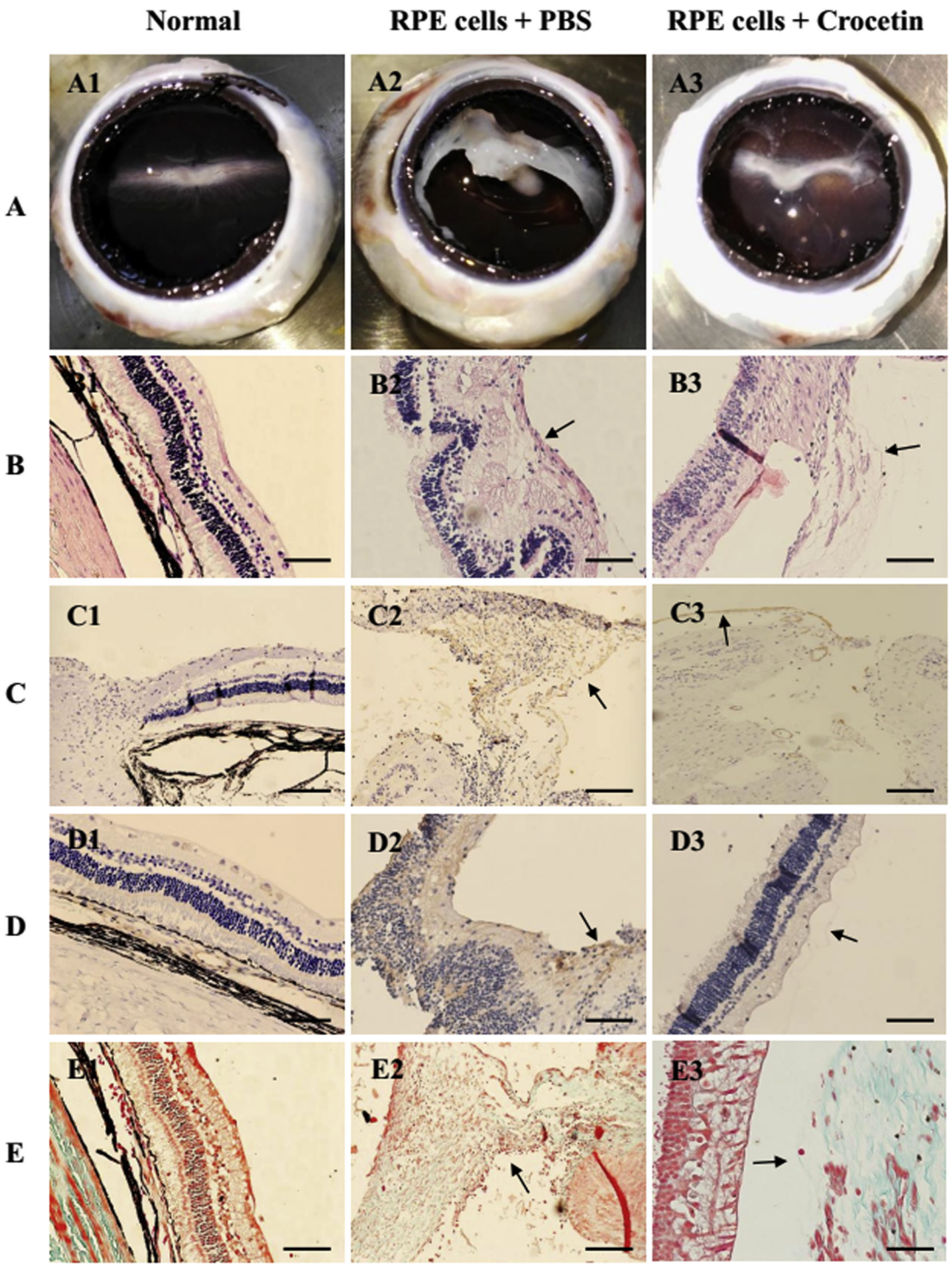

Fig. 5. Histopathological evaluation of the normal eyes and the eyes with PVR after treatment with ARPE-19 cells + PBS or ARPE-19 cells + 0.4 μmol crocetin. Normal eye: (A1) Macroscopic pathology of a normal eye. (B1) HE staining of a normal retina. (C1, D1) Immunohistochemical staining of normal retina and optic nerve for α-SMA. (E1) Masson's trichrome staining of a normal retina for collagen. The eye injected with ARPE-19 cells + PBS: (A2) Macroscopic pathology showed an infundibular retinal detachment. (B2) HE staining demonstrated a dense epiretinal membrane that wrinkled the retina. (C2) The fibrotic membranes mixed with many cells before the optic disc showed a prominent α-SMA expression. (D2) A completely detached retina showed disorganized retinal layers and a prominent α-SMA expression. (E2) Large amounts of collagen deposition mixed with many cells were present before the optic disc. ARPE-19 cells + 0.4 μmol crocetin: (A3) Macroscopic pathology showed localized detachment of the medullary ray and intravitreal membranes. (B3) HE staining presented a mild epiretinal membrane with a few cells. (C3) The thin fibrotic membranes in front of the optic disc showed a less prominent α-SMA expression than that in the eyes injected with PBS. (D3) The retina and thin epiretinal membranes demonstrated a weak α-SMA expression. (E3) Masson's trichrome staining showed a loosely arranged collagen mixed with a few cells. Scale bar: 50 μm.

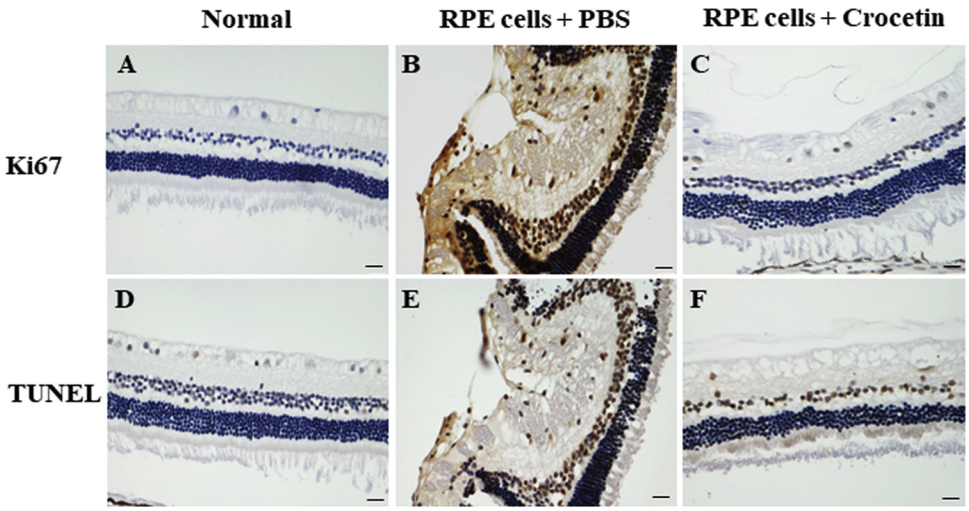

Fig. 6. Ki67 and TUNEL staining of the retinal sections in normal eyes and the eyes with PVR after treatment with ARPE-19 cells + PBS or ARPE-19 cells + 0.4 μmol crocetin. No TUNEL- and Ki67-positive cells were shown in normal eyes (A and D). Ki67 expression increased significantly in the eyes with PVR injected with ARPE-19 cells + PBS (B) compared with that injected with ARPE-19 cells + 0.4 μmol crocetin (C). TUNEL-positive cells were consistently shown in ganglion cell layer and inner nuclear layer in the two groups (E and F). Scale bar: 20 μm.

with ARPE-19 cells + 0.4 μmol crocetin showed a mild traction with formation of loose epiretinal membranes (Fig. 5B3). Immunohistochemistry results and Masson's trichrome stain showed a more prominent α-SMA expression and larger amounts of collagen deposition in the eyes injected with ARPE-19 cells + PBS than those injected with ARPE-19 cells + 0.4 μmol crocetin (Fig. 5C–E).

The expression of proliferative cell marker Ki67 increased significantly higher in the eyes injected with ARPE-19 cells + PBS compared with those injected with ARPE-19 cells + 0.4 μmol crocetin (Fig. 6B and C). The results of TUNEL assay indicated that there was no significant difference in TUNEL-positive cells between the two groups (Fig. 6E and F).

Representative baseline, 1- and 4-week scotopic and photopic ERG waveforms were shown in Fig. 7. In the group injected with ARPE-19 cells + PBS, there was a significant reduction in a-wave amplitudes at 1 and 4 weeks and a similar significant decrease in b-wave amplitudes at 4 weeks under both scotopic and photopic conditions. Scotopic and photopic b-wave amplitude reductions were slight at 1 week after injection. The group injected with ARPE-19 cells + 0.4 μmol crocetin showed a slight reduction in a- and b-wave amplitudes at 1 and 4 weeks in both scotopic and photopic 3.0 ERG.

4. Discussion

In the present study, a single intraocular injection of crocetin appears to be nontoxic to the retina, and HPLC analysis shows that the half-life of intravitreally administered crocetin is 4.231 h in the vitreous. Our results also demonstrate that intraocular crocetin significantly inhibits the development of PVR in a rabbit model injected with RPE cells.

Due to the difficulty of drug delivery to the retina in the form of topical eye drops or oral administration, we choose intravitreal injection as the primary method of drug administration to the ocular tissues (lens, iris, ciliary body, and retina). There were no signs of crocetin-related toxicity in either the retinal structure or function at a dosage of up to 0.4 μmol/eye (Fig. 1, Tables 1 and 2).

Subsequently, we investigated the pharmacokinetic properties of intravitreally injected crocetin in a rabbit model. At time zero, the vitreous was collected immediately after a single injection of 0.4 μmol (131.36 μg) of crocetin. Nearly one-third of the crocetin insolubly existed in the vitreous, one-third maintained a sufficiently solubilized concentration to inhibit RPE cell proliferation, migration and EMT according to our in vitro study, and the other one-third adhered to the surrounding ocular tissues (retina, ciliary body, and lens). The crocetin attained a maximum vitreous concentration after 1 h, and the levels were quantifiable up to 36 h after injection (Fig. 2, Table 3). After intravitreal administration, drug elimination may occur posteriorly through the blood-retina barrier to the choroidal blood circulation, which constitutes most of the ocular blood flow and anteriorly via aqueous humor turnover and uveal blood flow [23]. Drug elimination occurs after intravitreal injection primarily through anterior or posterior routes, depending on the drug's properties [23]. Crocetin is a lipophilic small molecule (328.4 Da) [13]. The pharmacokinetic properties of crocetin in the vitreous includes a short half-life (4.231 h). These results indicate that crocetin is mostly eliminated posteriorly.

PVR is characterized by the formation of contractile membranes within the vitreous and along the epiretinal and subretinal surfaces. Most PVR animal models have relied on the injection of external cells or factors reported in human PVR and often include other manipulations, such as gas compression and vitrectomy [2,24,25]. However, these models are flawed because they introduce large numbers of cells and do not take into account the early crucial steps in PVR development, including retinal break. Efforts have been directed toward developing models that more closely resemble the human pathophysiologic condition, placing more emphasis on the role of intraocular inflammation, wound healing, and the presence of growth factors than the introduction of external cells into the eye [10,26,27]. But those models usually involve surgical manipulation with reproducibility, to a large extent, depending on the operative skills of the surgeon. Existing experimental models of PVR all have limitations. We chose a cell injection method to establish PVR models due to its better reproducibility, safety, and stability compared with other methods such as lensectomy or retinal cryopexy with an ocular wound.

The ideal animal species of PVR should have a completely vascularized retina, similar to most mammals. Commonly used laboratory animals, such as rats and mice, have high retinal vascularization, a small eye and a relatively wide lens that makes manipulation to induce PVR difficult. We choose rabbits as the experimental animals for the relatively smaller size of the lens compared with the eyeball, which permits the manipulations easier without any damage to the lens/retina [28]. The retinas of rabbits are merangiotic, which indicates that blood vessels are present only in a small part of the retina and extend on the medullary ray in a horizontal direction. The medullary ray detachment simulates a retinal detachment in humans and shows PVR-like features [2].

In PVR, the mature RPE cells detach from Bruch's membrane, expose the vitreous factors, lose their epithelial characteristics, and undergo proliferation, migration, and epithelial-mesenchymal transition (EMT). Once the RPE cells transform into mesenchymal cells, such as fibroblasts and myofibroblasts, they express α-SMA, glial fibrillary acidic protein (GFAP), vimentin, secrete extracellular matrix proteins, contract, and become the main component of epiretinal membranes.

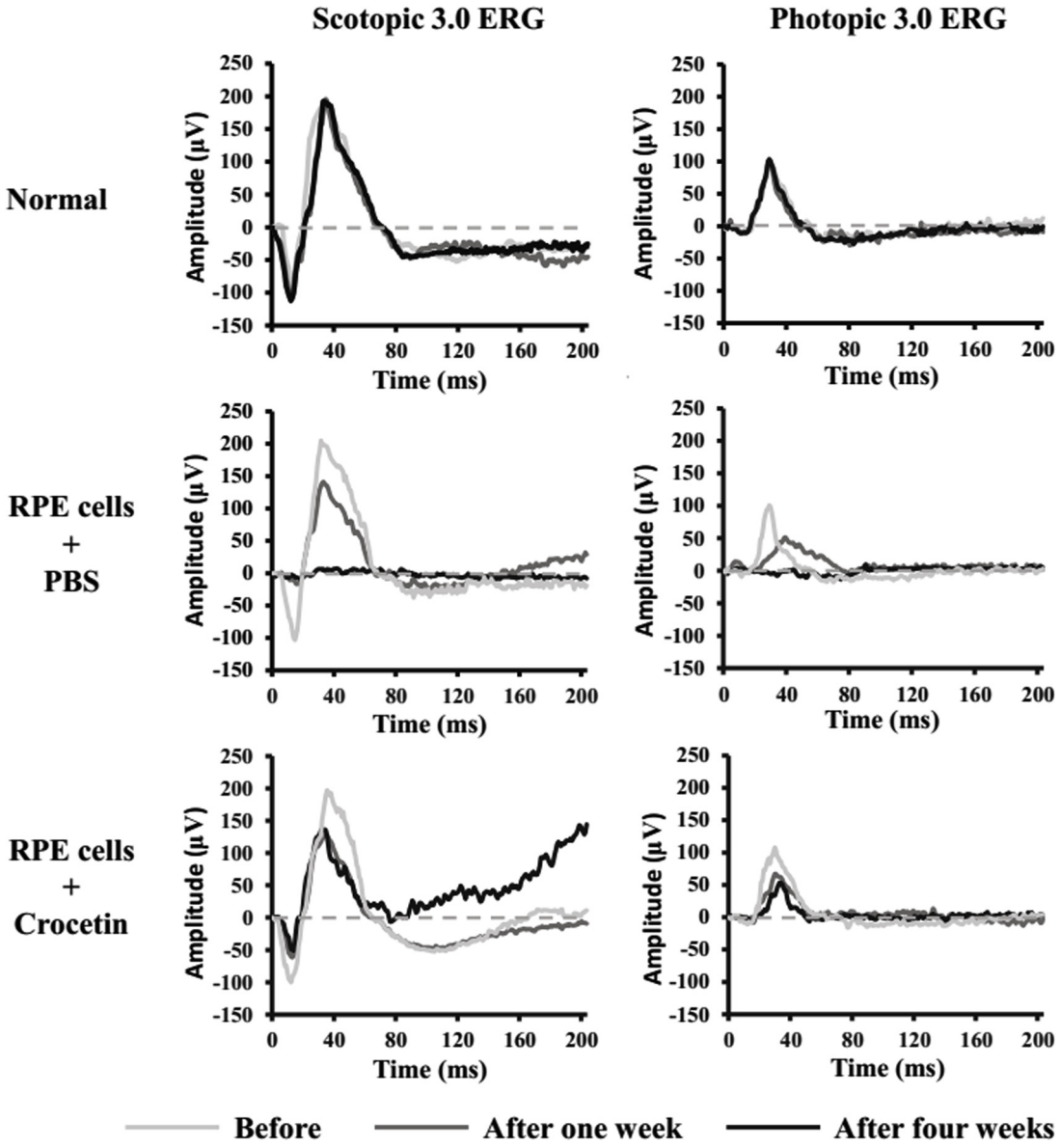

Fig. 7. Representative ERG waveforms of the normal eyes and the eyes injected with ARPE-19 cells + PBS or ARPE-19 cells + 0.4 μmol crocetin. Each series of responses shows the recordings pre-injection, 1 week post-injection and 4 weeks post-injection. A minor reduction in the amplitudes at 1-week post-injection in the two groups was sustained only in the eyes injected with ARPE-19 cells + 0.4 μmol crocetin at 4 weeks. A large reduction in amplitudes occurred 4 weeks after the injection of ARPE-19 cells + PBS.

Table 1
Mean scotopic A-Wave and B-Wave amplitudes.

	Baseline			Week 1			Week 2		
	R	L	P	R	L	P	R	L	P
Mean a-wave amplitude (S.D.) for animals treated with crocetin in the right eye and 0.4% DMSO in the left eye									
0.2 μmol	98 (14)	102 (13)	0.949	98 (12)	100 (13)	0.954	101 (17)	97 (7)	0.487
0.4 μmol	99 (8)	100 (15)	0.28	94 (11)	96 (9)	0.841	94 (6)	103 (10)	0.146
Mean b-wave amplitude (S.D.) for animals treated with crocetin in the right eye and 0.4% DMSO in the left eye									
0.2 μmol	318 (24)	307 (35)	0.276	298 (24)	308 (15)	0.383	300 (15)	298 (14)	0.723
0.4 μmol	292 (31)	314 (29)	0.595	292 (13)	301 (19)	0.762	304 (14)	308 (26)	0.201

Retinal detachment also triggers the proliferation of glial cells which results in the formation of a glial scar within the neural retina. Currently, vitrectomy remains the most effective treatment option for PVR [2]. However, although vitreoretinal surgical techniques have advanced over the last 20 years, the anatomical and visual outcomes are still unsatisfactory. These results indicate that there is a need to look for adjunctive approaches to prevent or halt the progression of PVR.

Crocetin effectively inhibits the progression of PVR in a RPE cell-induced rabbit model (Figs. 3–7). The pharmacological properties of crocetin make it well-suited for the potential treatment of PVR: (1) Crocetin demonstrates neuroprotective potential both in the central nervous system and retina through its anti-inflammatory effects and

Table 2
Mean photopic A-Wave and B-Wave amplitudes.

	Baseline			Week 1			Week 2		
	R	L	P	R	L	P	R	L	P
Mean a-wave amplitude (S.D.) for animals treated with crocetin in the right eye and 0.4% DMSO in the left eye									
0.2 µmol	12 (3)	11 (4)	0.49	9 (2)	10 (2)	0.66	14 (4)	13 (2)	0.186
0.4 µmol	14 (6)	12 (4)	0.443	10 (3)	12 (2)	0.092	14 (4)	13 (2)	0.299
Mean b-wave amplitude (S.D.) for animals treated with crocetin in the right eye and 0.4% DMSO in the left eye									
0.2 µmol	106 (15)	103 (24)	0.644	102 (12)	104 (18)	0.547	101 (15)	107 (16)	0.892
0.4 µmol	95 (27)	114 (29)	0.786	91 (14)	116 (9)	0.606	95 (16)	119 (22)	0.414

Table 3
Intraocular pharmacokinetics of crocetin.

Time point h	Vitreous humor µg/ml (S.D.)	Vitreous humor µM (S.D.)	Insoluble crocetin µg (S.D.)
0	35.13 (2.32)	106.97 (7.07)	41.56 (8.83)
1	36.77 (3.39)	111.98 (10.33)	20.37 (1.71)
3	30.82 (2.95)	93.86 (8.99)	11.71 (2.83)
7	11.13 (0.02)	33.89 (0.07)	3.48 (0.81)
12	4.06 (2.49)	12.36 (7.59)	0.59 (0.64)
24	1.89 (0.04)	5.77 (0.11)	0.92 (0.53)
36	0.09 (0.05)	0.27 (0.14)	0.03 (0.01)

inhibition of the caspase pathway [17,18,29]. Neuroprotection could not only improve the functional outcome after RD surgery by preventing photoreceptor death but could also be useful in preventing PVR. (2) Recently, strong evidence has shown that vitreous mediated indirect activation of PDGFRα results in prolonged activation of Akt, phosphorylation of Mdm2 and suppression of p53, which is an essential step in experimental PVR [25,30–32]. During our in vitro experiment, we observed that crocetin inhibited ARPE-19 cell proliferation and resulted in the accumulation of p53 [20]. The findings of the Retina 4 Project noted that the Pro variant of p53 codon 72 polymorphism results in an increased risk for developing PVR after a primary RD [33]. Here, we also found that crocetin could decrease the expression of proliferative cell marker Ki67 during PVR induction (Fig. 6). The research above indicates that crocetin, serving as an antiproliferative agent, could be proposed as a strategy directed toward preventing PVR. (3) The EMT of RPE cells is one of the primary concepts in the pathogenesis of PVR. Our previous study showed that crocetin could suppress the TGF-β_2-mediated EMT of ARPE-19 cells with an increased expression of ZO-1 and E-cadherin (epithelial markers) and a decreased expression of vimentin and α-SMA (mesenchymal markers) through the p38 MAPK pathway in an in vitro model of PVR [20]. In this study, as well as in a rabbit model of PVR, histological findings demonstrated that crocetin reduced fibrotic membrane formation and decreased α-SMA and collagen deposition in the epiretinal membranes (Figs. 4 and 5).

In conclusion, our data show that intravitreal crocetin appears to be nontoxic in rabbit eyes, and intraocular crocetin significantly inhibits the progression of PVR in a rabbit model. These results demonstrate that crocetin could work as a potential therapeutic agent to prevent the progression of PVR.

Conflictofinterest

The authors declare that there are no conflicts of interest

Acknowledgments

We thank Zhi-Qing Zhang and Ying Gong at the Department of Pharmacy, The Second Hospital of Hebei Medical University, for advice and technical assistance.

References

[1] W. Tseng, R.T. Cortez, G. Ramirez, S. Stinnett, G.J. Jaffe, Prevalence and risk factors for proliferative vitreoretinopathy in eyes with rhegmatogenous retinal detachment but no previous vitreoretinal surgery, Am. J. Ophthalmol. 137 (2004) 1105–1115, https://doi.org/10.1016/j.ajo.2004.02.008.
[2] J.C. Pastor, J. Rojas, S. Pastor-Idoate, S. Di Lauro, L. Gonzalez-Buendia, S. Delgado-Tirado, Proliferative vitreoretinopathy: a new concept of disease pathogenesis and practical consequences, Prog. Ret. Eye Res. 51 (2016) 125–155, https://doi.org/10.1016/j.preteyeres.2015.07.005.
[3] S. Pennock, L.J. Haddock, D. Eliott, S. Mukai, A. Kazlauskas, Is neutralizing vitreal growth factors a viable strategy to prevent proliferative vitreoretinopathy? Prog. Ret. Eye Res. 40 (2014) 16–34, https://doi.org/10.1016/j.preteyeres.2013.12.006.
[4] H. Ahmadieh, M. Feghhi, H. Tabatabaei, N. Shoeibi, A. Ramezani, M.R. Mohebbi, Triamcinolone acetonide in silicone-filled eyes as adjunctive treatment for proliferative vitreoretinopathy: a randomized clinical trial, Ophthalmology 115 (2008) 1938–1943, https://doi.org/10.1016/j.ophtha.2008.05.016.
[5] P.E. Rubsamen, S.W. Cousins, Therapeutic effect of periocular corticosteroids in experimental proliferative vitreoretinopathy, Retina 17 (1997) 44–50.
[6] A. Sadaka, G.P. Giuliari, Proliferative vitreoretinopathy: current and emerging treatments, Clin. Ophthalmol. 6 (2012) 1325–1333, https://doi.org/10.2147/OPTH.S27896.
[7] HirookaK. Du YH, O. Miyamoto, Y.Q. Bao, B. Zhang, J.B. An, J.X. Ma, Retinoic acid suppresses the adhesion and migration of human retinal pigment epithelial cells, Exp. Eye Res. 109 (2013) 22–30, https://doi.org/10.1016/j.exer.2013.01.006.
[8] G. Velez, A.R. Weingarden, H. Lei, A. Kazlauskas, G. Gao, SU9518 inhibits proliferative vitreoretinopathy in fibroblast and genetically modified Muller cell-induced rabbit models, Invest. Ophthalmol. Vis. Sci. 54 (2013) 1392–1397, https://doi.org/10.1167/iovs.12-10320.
[9] Y. Zheng, Y. Ikuno, M. Ohj, S. Kusaka, R. Jiang, O. Cekiç, M. Sawa, Y. Tano, Platelet-derived growth factor receptor kinase inhibitor AG1295 and inhibition of experimental proliferative vitreoretinopathy, Jpn. J. Ophthalmol. 47 (2003) 158–165.
[10] K. Nassar, S. Grisanti, A. Tura, J. Lüke, M. Lüke, M. Soliman, S. Grisanti, A TGF-beta receptor 1 inhibitor for prevention of proliferative vitreoretinopathy, Exp. Eye Res. 123 (2014) 72–86, https://doi.org/10.1016/j.exer.2014.04.006.
[11] D.G. Charteris, G.W. Aylward, D. Wong, C. Groenewald, R.H. Asaria, C. Bunce, A randomized controlled trial of combined 5-fluorouracil and low-molecular-weight heparin in management of established proliferative vitreoretinopathy, Ophthalmology 111 (2004) 2240–2245, https://doi.org/10.1016/j.ophtha.2004.05.036.
[12] K. Ishikawa, S. He, H. Terasaki, H. Nazari, H. Zhang, C. Spee, R. Kannan, D.R. Hinton, Resveratrol inhibits epithelial-mesenchymal transition of retinal pigment epithelium and development of proliferative vitreoretinopathy, Sci. Rep. 5 (2015) 16386, https://doi.org/10.1038/srep16386.
[13] G. William, G.R. Gutheil, R. Amitabha, D. Animesh, Crocetin: an agent derived from saffron for prevention and therapy for cancer, Curr. Pharm. Biotechnol. 13 (2012) 173–179.
[14] P. Rangarajan, D. Kwatra, S. Ramalingam, et al., Crocetinic acid inhibits hedgehog signaling to inhibit pancreatic cancer stem cells, Oncotarget 6 (2015) 27661–27673, https://doi.org/10.18632/oncotarget.4871.
[15] S. Li, S. Jiang, W. Jiang, Y. Zhou, X.Y. Shen, T. Luo, L.P. Kong, H.Q. Wang, Anticancer effects of crocetin in human esophageal squamous cell carcinoma KYSE-150 cells, Oncol. Lett. 9 (2015) 1254–1260, https://doi.org/10.3892/ol.2015.2869.
[16] P. Ray, D. Guha, J. Chakraborty, S. Banerjee, A. Adhikary, S. Chakraborty, T. Das, G. Sa, Crocetin exploits p53-induced death domain (PIDD) and FAS-associated death domain (FADD) proteins to induce apoptosis in colorectal cancer, Sci. Rep. 6 (2018) 32979, https://doi.org/10.1038/srep32979.
[17] F. Ishizuka, M. Shimazawa, N. Umigai, H. Ogishima, S. Nakamura, K. Tsuruma, H. Hara, Crocetin, a carotenoid derivative, inhibits retinal ischemic damage in mice, Eur. J. Pharmacol. 703 (2013) 1–10, https://doi.org/10.1016/j.ejphar.2013.02.007.
[18] Y. Ohno, T. Nakanishi, N. Umigai, K. Tsuruma, M. Shimazawa, H. Hara, Oral administration of crocetin prevents inner retinal damage induced by N-methyl-D-aspartate in mice, Eur. J. Pharmacol. 690 (2012) 84–89, https://doi.org/10.1016/j.ejphar.2012.06.035.
[19] Y. Song, L. Zhu, M. Li, Antifibrotic effects of crocetin in scleroderma fibroblasts and in bleomycin-induced sclerotic mice, CLINICS 68 (2013) 1350–1357, https://doi.org/10.6061/clinics/2013(10)10.

[20] H.F. Wang, J.X. Ma, Q.L. Shang, J.B. An, H.T. Chen, Crocetin inhibits the proliferation, migration and TGF-beta2-induced epithelial-mesenchymal transition of retinal pigment epithelial cells, Eur. J. Pharmacol. 815 (2017) 391–398, https://doi.org/10.1016/j.ejphar.2017.09.041.
[21] M.F. Marmor, A.B. Fulton, G.E. Holder, Y. Miyake, M. Brigell, M. Bach, ISCEV Standard for full-field clinical electroretinography (2008 update), Doc. Ophthalmol. 118 (2009) 69–77, https://doi.org/10.1007/s10633-008-9155-4.
[22] D.M. Fastenberg, K.R. Diddie, J.M. Delmage, K. Dorey, Intraocular injection of silicone oil for experimental proliferative vitreoretinopathy, Am. J. Ophthalmol. 95 (1983) 663–667.
[23] E.M. Del Amo, A. Urtti, Rabbit as an animal model for intravitreal pharmacokinetics: clinical predictability and quality of the published data, Exp. Eye Res. 137 (2015) 111–124, https://doi.org/10.1016/j.exer.2015.05.003.
[24] G. Ma, Y. Duan, X. Huang, et al., Prevention of proliferative vitreoretinopathy by suppression of phosphatidylinositol 5-Phosphate 4-Kinases, Invest. Ophthalmol. Vis. Sci. 57 (2016) 3935–3943, https://doi.org/10.1167/iovs.16-19405.
[25] G. Zhou, Y. Duan, G. Ma, et al., Introduction of the MDM2 T309G mutation in primary human retinal epithelial cells enhances experimental proliferative vitreoretinopathy, Invest. Ophthalmol. Vis. Sci. 58 (2017) 5361–5367, https://doi.org/10.1167/iovs.17-22045.
[26] K. Umazume, Y. Barak, K. McDonald, L. Liu, H.J. Kaplan, S. Tamiya, Proliferative vitreoretinopathy in the Swine-a new model, Invest. Ophthalmol. Vis. Sci. 53 (2012) 4910–4916, https://doi.org/10.1167/iovs.12-9768.
[27] R. Hoerster, P.S. Muether, S. Vierkotten, M.M. Hermann, B. Kirchhof, S. Fauser, Upregulation of TGF-ß1 in experimental proliferative vitreoretinopathy is accompanied by epithelial to mesenchymal transition, Graefes Arch. Clin. Exp. Ophthalmol. 252 (2014) 11–16, https://doi.org/10.1007/s00417-013-2377-5.
[28] R.N. Agrawal, S. He, C. Spee, J.Z. Cui, S.J. Ryan, D.R. Hinton, In vivo models of proliferative vitreoretinopathy, Nat. Protoc. 2 (2007) 67–77, https://doi.org/10.1038/nprot.2007.4.
[29] K.N. Nam, Y.M. Park, H.J. Jung, et al., Anti-inflammatory effects of crocin and crocetin in rat brain microglial cells, Eur. J. Pharmacol. 648 (2010) 110–116, https://doi.org/10.1016/j.ejphar.2010.09.003.
[30] H. Lei, A. Kazlauskas, Growth factors outside of the platelet-derived growth factor (PDGF) family employ reactive oxygen species/Src family kinases to activate PDGF receptor alpha and thereby promote proliferation and survival of cells, J. Biol. Chem. 284 (2009) 6329–6336, https://doi.org/10.1074/jbc.M808426200.
[31] H. Lei, M.A. Rheaume, G. Velez, S. Mukai, A. Kazlauskas, Expression of PDGFRalpha is a determinant of the PVR potential of ARPE19 cells, Invest. Ophthalmol. Vis. Sci. 52 (2011) 5016–5021, https://doi.org/10.1167/iovs.11-7442.
[32] H. Lei, G. Velez, A. Kazlauskas, Pathological signaling via platelet-derived growth factor receptor {alpha} involves chronic activation of Akt and suppression of p53, Mol. Cell. Biol. 31 (2011) 1788–1799, https://doi.org/10.1128/MCB.01321-10.
[33] S. Pastor-Idoate, I. Rodriguez-Hernandez, J. Rojas, et al., The p53 codon 72 polymorphism (rs1042522) is associated with proliferative vitreoretinopathy: the Retina 4 Project, Ophthalmology 120 (2013) 623–628, https://doi.org/10.1016/j.ophtha.2012.08.019.